than in the less "polar" but better σ-donating tetrahydrofuran, and (iii) in acetonitrile than in the less "polar" but better σ- and π-donating acetone (Figures 6 and 7).

These results, especially point i, suggest a π type donor interaction (Chart V) between solvent molecules and a complex such as $(TCNE)M(CO)_5$ ("π solvates"); conventional donor numbers (DN) derived from complexes $Cl_5Sb{\cdot}S$ (S = solvent)[29,53] make only allowance for σ type interactions and do not seem to be applicable here (Table III).

A solvent parameter scale for π type interactions remains to be constructed;[54] such information should be valuable to all organometallic chemistry (including catalysis[1]) that makes use of π-coordinating ligands.

While no band structure was observed for the long-wavelength charge-transfer band of **7**, the tungsten analogue **8** displays a high-energy shoulder and a low-energy separate band in solvents of very low polarity (Figure 4). In agreement with previous arguments[30b-d,34,40] we assign these additional features to differently polarized transitions from the three split levels in a low-spin d^6 system; expectedly, this splitting is much smaller for Cr than for the heavier homologue W. The larger and perhaps less symmetrically coordinated[25] TCNQ π complexes **9** and **10** exhibit band structure in all solvents (Figure 5), which may in part be attributed to the presence of an IL transition of the TCNQ anion radical (ν = 11 880 cm^{-1}).[55] Infrared spectra of such solutions do not show significant amounts of dissociated TCNQ or $M(CO)_5$ solvent adducts;[25] there is, however, slow formation of $TCNQ^{\bullet-}$ in acetonitrile with its high dielectric constant[29] (cf. eq 5).

Summary. This work illustrates the intriguing variability of geometrical (σ and π coordination) and electronic structures for complexes of polynitrile acceptor ligands with transition-metal carbonyl fragments. The compounds discussed show a continuous change from systems with MLCT to those with LMCT character of the major long-wavelength transitions, depending on the back-bonding capability of coordinated d^6 metal fragments.[56] Electrochemistry, reactivity, and ESR and vibrational (ν_{CN}, ν_{CO}, ν_{CC}) as well as charge-transfer spectroscopy indicate the considerably but not completely[8] reduced nature of ligands such as TCNE or TCNQ and the weak covalent bonding in such complexes. The equally important chemical consequences of this situation, viz., the enhanced nucleophilicity of the tetradentate ligands, has only begun to be exploited, e.g. in the formation of novel tetranuclear complexes with remarkable properties.[14,57]

Acknowledgment. Support for this work has come from Deutsche Forschungsgemeinschaft, Stiftung Volkswagenwerk, Flughafen Frankfurt/Main AG, Hermann-Willkomm-Stiftung, and BASF AG. We are grateful to Professor K. Wieghardt and Dr. K. Pohl (Bochum, FRG) for near-IR measurements and to Professor S. Hünig (Würzburg, FRG) for a gift of 2,5-DM-DCNQI.

(53) Gutmann, V. *The Donor-Acceptor Approach to Molecular Interactions*; Plenum: New York, 1978.
(54) Kaim, W.; Olbrich-Deussner, B. Work in progress.
(55) Acker, D. S.; Hertler, W. R. *J. Am. Chem. Soc.* **1962**, *84*, 3370. Melby, L. R.; Harder, R. J.; Hertler, W. R.; Mahler, W.; Benson, R. E.; Mochel, W. E. *J. Am. Chem. Soc.* **1962**, *84*, 3374.
(56) Morris, R. H.; Earl, K. A.; Luck, R. L.; Lazarowych, N. J.; Sella, A. *Inorg. Chem.* **1987**, *26*, 2674.
(57) Jørgensen, C. K. *Oxidation Numbers and Oxidation States*; Springer-Verlag: Berlin, 1969.
(58) Richert, S. A.; Tsang, P. K. S.; Sawyer, D. T. *Inorg. Chem.* **1988**, *27*, 1814.
(59) Gross, R. Ph.D. Thesis, University of Frankfurt, 1987. Schulz, A. Ph.D. Thesis, University of Stuttgart, 1989.

Contribution from the Department of Chemistry, The University of Chicago, 5735 South Ellis Avenue, Chicago, Illinois 60637, and University Chemical Laboratories, University of Cambridge, Lensfield Road, Cambridge CB2 1EW, U.K.

Bonding in Transition-Metal Clusters

David J. Wales*,† and Anthony J. Stone‡

Received January 27, 1989

In this paper, the application of Stone's tensor surface harmonic (TSH) theory to the bonding in transition-metal clusters is reviewed and developed by using specific examples and comparisons with previous studies. The relationship between TSH theory and the isolobal principle is described with the aid of Fenske–Hall calculations on some small transition-metal clusters. A detailed analysis of the results for $Ru_5(CO)_{15}^{2-}$ shows that the sets of orbitals expected from TSH theory are all clearly identifiable. The application of the method to nonconical cluster vertices, clusters with interstitial atoms, and some interesting metallaboranes is also discussed. Clusters with a vertex lying on an idealized principal rotation axis are particularly interesting; their electron counts and the effects of low symmetry are considered.

Introduction

The problem of understanding the electron counts in both main-group and transition metal clusters has been investigated extensively for many years. The debor principle, which emerged in the early 1970s from the work of Williams,[1] Wade,[2] and Rudolph,[3] first systemized the correlation between structure and electron counts for closo, nido, and arachno boranes. The isolobal principle, which allows transition-metal clusters to be understood in terms of the simpler borane structures, has also proved very useful.[4] The term polyhedral skeletal electron pair theory was later introduced to cover the correlation between electron count and cluster structure.[5] Its development has often been facilitated by means of extended Hückel calculations.[6] More recently Stone's tensor surface harmonic (TSH) theory[7] has been used to provide a firmer theoretical foundation for these generalizations.[8,9]

In the TSH model, approximate linear combinations of atomic orbitals are formed by using the eigenfunctions for the particle on a sphere problem (the spherical harmonics) and the tensor surface harmonics. By analogy with the relation between the Hückel wave functions for cyclic polyenes and the eigenfunctions

† The University of Chicago.
‡ University of Cambridge.

(1) Williams, R. E. *Prog. Boron Chem.* **1970**, *2*, 51. Williams, R. E. *Inorg. Chem.* **1971**, *10*, 210. Williams, R. E. *Adv. Inorg. Chem. Radiochem.* **1976**, *18*, 67.
(2) Wade, K. *J. Chem. Soc., Chem. Commun.* **1971**, 792.
(3) Rudolph, R. W.; Pretzer, W. R. *Inorg. Chem.* **1972**, *11*, 1974. Rudolph, R. W. *Acc. Chem. Res.* **1976**, *9*, 446.
(4) Hoffmann, R. *Angew. Chem., Int. Ed. Engl.* **1982**, *21*, 711.
(5) Mason, R.; Thomas, K. M.; Mingos, D. M. P. *J. Am. Chem. Soc.* **1973**, *95*, 3802.
(6) Hoffmann, R.; Lipscomb, W.N. *J. Chem. Phys.* **1962**, *36*, 2179. Hoffmann, R. *J. Chem. Phys.* **1963**, *39*, 1397.
(7) Stone, A. J. *Mol. Phys.* **1980**, *41*, 1339. Stone, A. J. *Inorg. Chem.* **1981**, *20*, 563. Stone, A. J.; Alderton, M. J. *Inorg. Chem.* **1982**, *21*, 2297. Stone, A. J. *Polyhedron* **1984**, *3*, 1299.
(8) Mingos, D. M. P.; Johnston, R. L. *Struct. Bonding* **1987**, *68*, 29.
(9) Fowler, P. W.; Porterfield, W. W. *Inorg. Chem.* **1985**, *24*, 3511. Fowler, P. W. *Polyhedron* **1985**, *4*, 2051.

0020-1669/89/1328-3120$01.50/0

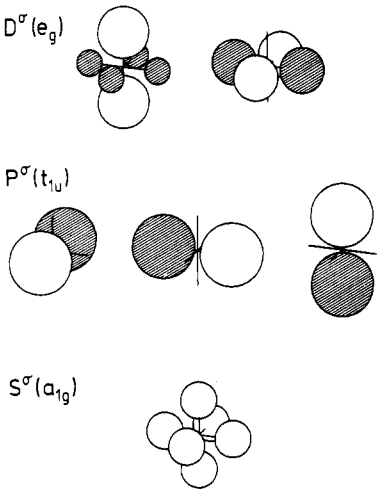

Figure 1. The six s^{σ} cluster orbitals of an octahedron.

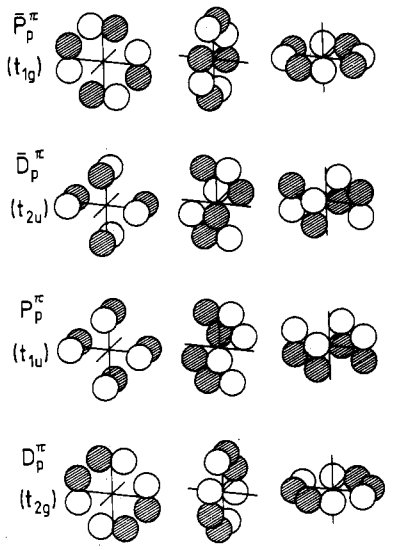

Figure 2. p^{π} cluster orbitals of an octahedral cluster. Note the relationships between the partner odd and even orbitals.

for the particle on a ring problem, we expect these linear combinations to be reasonable first-order approximations to the actual cluster orbitals. Many useful results may be derived by using this formalism, particularly the rationalization of cluster electron counts; the reader is referred elsewhere for details.[7] More recently, we have investigated the effects of the detailed arrangement of the vertex atoms on the TSH bonding model and found that many of the most useful results of the original method remain valid.[10] We have also used the model in our investigations of structural rearrangements in main-group clusters, deriving some useful symmetry rules and explaining the relative fluxionalities of these systems.[11]

Although TSH theory in its original form enabled the general $7n + 1$ occupied orbitals of a simple transition-metal cluster carbonyl to be identified, the large number of orbitals involved makes it harder to use than for main-group clusters, and the predictions are less clear-cut. In this account, we show how TSH theory and the isolobal principle are related, and use this insight to strengthen our understanding of the bonding in transition-metal clusters. In effect, this scheme represents a unification of the concepts of isolobality, local site symmetry,[12] and the fragment molecular approach.[13]

Summary of Tensor Surface Harmonic Theory

TSH theory is essentially an approximate symmetry classification. A cluster is treated as if it were spherical, and the appropriate symmetry labels for spherical symmetry are the angular momentum quantum numbers L and M, as in an atom. There is also a parity classification: functions may be changed in sign or unchanged by inversion. The prototype functions that can be classified in this way are the spherical harmonics, Y_{LM}, which have even or odd parity under inversion for L even or odd respectively.

TSH theory classifies the basis functions of each cluster atom into σ, π, and δ orbitals having respectively 0, 1, and 2 nodal planes containing the radius vector from the center of the cluster to the atom. Cluster orbitals are formed from the σ basis functions σ_i (where the index i labels the cluster atoms) by using the values of spherical harmonics evaluated at the cluster vertices as expansion coefficients. That is, the cluster orbital ψ^{σ}_{LM} is a linear combination of the form

$$\psi^{\sigma}_{LM} = \sum_i Y_{LM}(\theta_i,\phi_i)\ \sigma_i$$

where θ_i and ϕ_i are the spherical color coordinates of the cluster atom. The sets of ψ^{σ}_{LM} with $L = 0, 1, 2, \ldots$ are denoted S^{σ}, P^{σ}, D^{σ}, ..., while the whole set is collectively denoted L^{σ}. For a real cluster, these labels do not describe genuine symmetry characteristics, but the approximate classification is very valuable nevertheless. If the molecular orbitals are expressed in terms of ψ^{σ}_{LM}, rather than the original atomic σ orbitals, we can expect to find, and in fact do find, that functions of different L or M do not mix with each other very strongly. To this extent, the ψ^{σ}_{LM} are good approximations to the molecular orbitals themselves. The six σ orbitals for the octahedron are illustrated in Figure 1.

However, this is not the whole story. So far we have dealt only with the σ orbitals of the cluster atoms, and we need a way to handle the π and σ orbitals. To do this, we derive from the surface harmonics two sets of *vector surface harmonics* $\mathbf{V}_{LM}$ and $\bar{\mathbf{V}}_{LM}$, defined by

$$\mathbf{V}_{LM} = \nabla Y_{LM} \qquad \bar{\mathbf{V}}_{LM} = \mathbf{r} \times \mathbf{V}_{LM} = \mathbf{r} \times \nabla Y_{LM}$$

From each Y_{LM}, we obtain in this way two vector functions. Both of them are tangential to the surface of the sphere. $\mathbf{V}_{LM}$ has the same parity as the parent Y_{LM}, and may be called a *polar* (or even) vector surface harmonic. $\bar{\mathbf{V}}_{LM}$ has the opposite parity (that is, it changes sign under inversion if L is even and is unchanged if L is odd) and may be called an *axial* (or odd) vector surface harmonic.

The direction and magnitude of the polar vector surface harmonic $\mathbf{V}_{LM}$ at cluster atom i are used to give the magnitude and direction of a π-orbital contribution to a π-type cluster orbital ψ^{π}_{LM} with the same parity as the parent Y_{LM}. In the same way $\bar{\mathbf{V}}_{LM}$ yields a cluster orbital $\bar{\psi}^{\pi}_{LM}$ with the opposite parity. There is no vector surface harmonic with $L = 0$, because Y_{00} is constant and its derivative is zero, so there is no S^{π} cluster orbital, but there are P^{π}, D^{π}, ... orbitals derived from the polar vector surface harmonics, and $\bar{P}^{\pi}$, $\bar{D}^{\pi}$, ... orbitals derived from the axial ones. These two sets are denoted generically by the symbols L^{π} and $\bar{L}^{\pi}$ respectively.

An important feature is that there is a pairing relation between the orbitals ψ^{π}_{LM} and $\bar{\psi}^{\pi}_{LM}$. Each of these may be obtained from the other by rotating the π-orbital contribution of each atom by 90° about the radius vector to that atom, all in the same direction. Repetition of this procedure recovers the original function except for a change of sign. It also turns out that this pairing operation converts bonding interactions into antibonding ones and vice versa.[7] Indeed, it is after the case that the L^{π} orbitals are bonding and the $\bar{L}^{\pi}$ ones are antibonding, especially for deltahedral clusters, in which all the faces are triangular. All the π cluster orbitals for the octahedron are illustrated in Figure 2. The usual electron count for closo clusters follows from the fact that the occupied orbitals are usually the n orbitals of the bonding L^{π} set (or combinations of these with the L^{σ} orbitals of the same symmetry) together with the strongly bonding S^{σ} orbital.

(10) Stone, A. J.; Wales, D. J. *Mol. Phys.* **1987**, *61*, 747.
(11) Wales, D. J.; Stone, A. J. *Inorg. Chem.* **1987**, *26*, 3845. Wales, D. J.; Mingos, D. M. P.; Zhenyang, L. *Inorg. Chem.*, in press. Wales, D. J.; Mingos, D. M. P. *Polyhedron*, in press.
(12) Rytter, E. *Chem. Phys.* **1976**, *12*, 355.
(13) Evans, D. G. *J. Chem. Soc., Chem. Commun.* **1983**, 675.

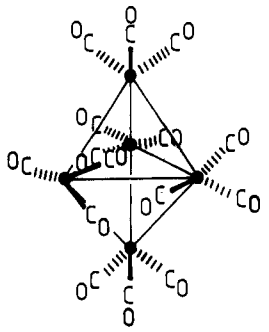

Figure 3. Idealized geometry used for the calculations on $Ru_5(CO)_{15}^{2-}$.

In certain structures, however, it happens that there is a degenerate pair of orbitals that are paired with each other, and then the fact that bonding and antibonding characteristics are exchanged by the pairing operation means that both of them must be nonbonding. This phenomenon occurs in tetrahedral molecules with an odd number of sets of four equivalent atoms, and in molecules in which there is an odd number of atoms on a symmetry axis of order 3 or more.[9] This results in a modification of the normal electron-counting rules: if the non-bonding pair is occupied, then there are $n + 2$ occupied cluster orbitals, and if it is vacant, there are only n. A total of $n + 1$ is not possible, because that would require the degenerate pair to be only half-occupied.

In transition-metal clusters, we have to deal with δ atomic orbitals as well as σ and π. These are handled by a further extension of TSH theory, using *tensor surface harmonics*, which are second derivatives of Y_{LM}. These too comprise polar harmonics with the same parity as Y_{LM} and axial ones with the opposite parity, and there is a pairing operation that relates the one to the other. However, it appears that they are not greatly involved in the bonding in simple transition metal-cluster carbonyls. In the present paper, we refer to these cluster orbitals collectively as L^{δ} and $\bar{L}^{\delta}$ functions and will not need to enquire into them more closely.

Analysis of $Ru_5(CO)_{15}^{2-}$

First, it will be instructive to consider some Fenske–Hall calculations on simple transition metal carbonyl clusters. The Fenske–Hall method[14] is an ab initio SCF technique in which some of the integrals are evaluated approximately by using a point-charge model and Mulliken population analyses.[15] One particularly useful feature of our program for the present application is the ability to transform the basis functions into the TSH linear combinations. The cluster orbital basis was constructed by transforming the required spherical harmonic derivatives in global axes to local axes; the chain rule and the properties of the unit base vectors of orthogonal coordinate systems were used.

Calculations were performed on $Ru_5(CO)_{15}^{2-}$ by using optimized exponents for the minimal Slater-type-orbital basis calculated for the ground state of the ruthenium atom.[16] The C–Ru–C angles were all set equal to 90°, and the Ru–C–O angles were set to 180° (Figure 3). The results illustrated in Figure 4 are for the C_{3h} geometry in which three carbonyls lie in the equatorial plane with Ru–Ru = 2.75 Å, Ru–CO = 1.9 Å, and C–O = 1.16 Å. Several calculations were performed in which the bond lengths and carbonyl positions were varied. A larger HOMO–LUMO gap is found on decreasing the Ru–Ru and Ru–CO distances from those used for Figure 4, and the frontier region is shifted to lower energy; however, the important features for the present purpose are always present at sensible geometries.

All the predicted TSH theory features are easily identifiable in the molecular orbitals, and in order of ascending energy we find the following: (a) 15 carbonyl σ bonds (−34.55 to −34.00 eV); (b) 15 CO oxygen lone pairs (−15.79 to −14.51 eV); (c) 30

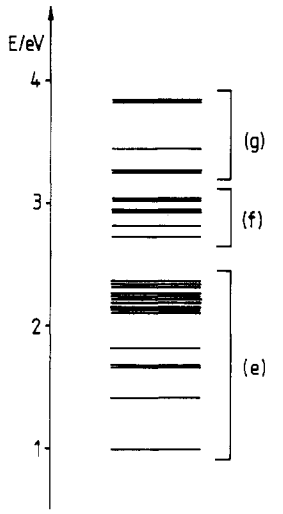

Figure 4. Results of a Fenske–Hall calculation on $Ru_5(CO)_{15}^{2-}$ showing the TSH features of the frontier region. Sets e–g are described in the text.

carbonyl π orbitals (−13.39 to −12.36 eV); (d) 15 orbitals corresponding to Ru–CO bonding which are mostly CO carbon lone pair in character (60–70%) (−11.21 to −7.26 eV); (e) 15 Ru orbitals with varying degrees of carbonyl π^* character, consisting of $S^{\sigma}_{s/p}$, four d^{σ} and ten d^{δ} functions (1.00 to 2.37 eV); (f) 6 cluster bonding (occupied) frontier orbitals, 5 of which are composed mostly of metal d^{π} orbitals with some carbonyl π^* character while the other is 80% S^{σ}_{d}, 10% S^{σ}_{p}, and 7% S^{σ}_{s} [at shorter bond lengths this orbital is the HOMO, as observed in extended Hückel calculations][17] (2.73 to 3.04 eV); (g) 5 cluster antibonding (vacant) frontier orbitals composed mostly of metal d^{π} with some carbonyl π^* character (3.24 to 3.83 eV); (h) 30 carbonyl π^* orbitals with varying degrees of metal character (5.63 to 10.78 eV); (i) 4 orbitals mainly composed of s^{σ} and p^{σ} metal functions (19.30 to 40.37 eV); (j) 10 Ru–CO antibonding orbitals, which are mainly metal p^{π} (40.70 to 64.64 eV); (k) 5 Ru–CO antibonding orbitals, which are mainly metal s^{σ} and p^{σ} (73.08 to 82.31 eV); (l) 15 carbonyl σ-antibonding orbitals (125.31 to 149.62 eV). It is a simple matter to distinguish the TSH theory sets of orbitals from the above picture. The accessible cluster orbitals are identified as S^{σ}, the HOMO, and a complete set of five L^{π}_{p}/L^{π}_{d} orbitals (f), all the L^{δ}_{d} and $\bar{L}^{\delta}_{d}$ orbitals plus a complete set of five L^{σ}_{d} orbitals (all mixed with carbonyl π^*) (e), and 15 metal–carbonyl bonding orbitals, which are actually mostly carbonyl in character (d). The inaccessible cluster orbitals are simply a set of five $\bar{L}^{\pi}_{p}/\bar{L}^{\pi}_{d}$ orbitals (g) and four inwardly hybridized $L^{\sigma}_{p}/L^{\sigma}_{s}$ orbitals (i), which represent one complete set of σ functions, except for the S^{σ} member, which is the HOMO. The clear distinction between these sets is an excellent vindication of the TSH description of the electronic structure of these systems, and may be compared with Evans' schematic diagram.[17]

We can now relate the orbitals of conical fragments from the isolobal viewpoint to the TSH orbitals. The three isolobal cluster bonding orbitals per vertex are equivalent to (that is, can be transformed into) one σ and two π orbitals in TSH notation, which give rise to the $n + 1$ occupied orbitals of set f and the $2n - 1$ inaccessible orbitals in sets g and i. The three t_{2g} "unhybridized" orbitals per vertex correspond to all the δ orbitals and a complete set of $L^{\sigma}_{z^2}$ orbitals, i.e. in local axes the $d_{x^2-y^2}$, d_{xy}, and d_{z^2} orbitals. The remaining $3n$ metal orbitals are outwardly hybridized and interact strongly with the ligands to give $3n$ accessible metal–carbonyl bonding orbitals.

Although these results are very satisfying from the TSH viewpoint, it is most important to realize that *the theory does not depend at all upon any approximate calculations*; these are simply used for illustration. The method is based upon symmetry principles, and our conclusions support Woolley's view that the isolobal

(14) Hall, M. B.; Fenske, R. F. *Inorg. Chem.* **1972**, *11*, 768.
(15) Mulliken, R. S. *J. Chem. Phys.* **1955**, *23*, 1833, 1841.
(16) Clementi, E.; Raimondi, D. L.; Reinhardt, W. P. *J. Chem. Phys.* **1967**, *47*, 1300.
(17) Evans, D. G. *Inorg. Chem.* **1986**, *25*, 4602.

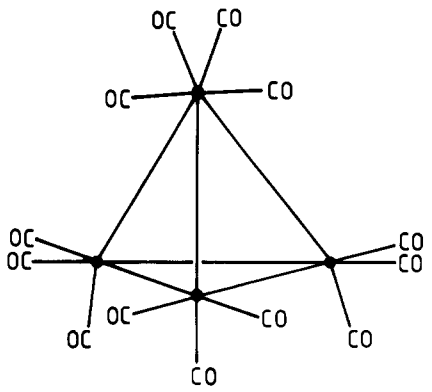

Figure 5. $Os_4(CO)_{13}$. The osmium atoms define the vertices of the tetrahedron.

principle follows fundamentally from symmetry considerations.[18] We emphasize this because of the rather controversial nature of any calculations upon transition-metal clusters.

Nonconical Structures

Let us now consider $Os_4(CO)_{13}^{2-}$, which is illustrated in Figure 5. This is a 60-electron species (here and below we count only the valence electrons of interest) whose bonding may be rationalized as follows. There are 13 Os–CO σ bonds, and if each metal uses three orbitals for cluster bonding, there remain 11 "unhybridized" occupied orbitals. Six additional Os–Os edge-bonds give a total of 30 accessible orbitals, as required. There are several points of interest in this analysis. First, we note that the molecule has a cluster bonding orbital count of $n + 2 = 6$. This may be interpreted in terms of edge bonding, as above, but an alternative viewpoint is to note that the tetrahedron is one of the structures mentioned above for which there is a nonbonding pair of cluster orbitals, so that the number of occupied cluster orbitals has to be either n or $n + 2$ and not $n + 1$.

The most important observation is that the nonconical fragment uses three orbitals for cluster bonding, the same number as the conical fragments above. These three hybrids correspond in TSH theory to the $3n$ inwardly hybridized orbitals (one σ and two π orbitals per vertex atom) which generate the $n + 1$ (or n or $n + 2$, etc.) cluster bonding orbitals. The remaining $6n$ metal orbitals all correlate with accessible orbitals, independent of the precise distribution of ligands. This is clearly true in the above molecule; effectively an "unhybridized" Os orbital has been used to bond to the extra carbonyl and is occupied by two electrons as it would be in a conical fragment. The relation to the isolobal approach[1,19] is immediately apparent, and we can conclude that the isolobal method will work whenever the assumed TSH theory hybridization scheme is appropriate. Exceptions arise when each vertex cannot contribute two π orbitals for skeletal bonding, and examples are $[Os(CO)_4]_3$ (triangular) and clusters composed of PtL_2 fragments. In these cases all the vertices are isolobal to CH_2 fragments, and more detailed considerations are required.[20] A detailed critique of cluster hybridization schemes is given elsewhere.[21]

The utility of the above method may be illustrated by some further examples. First we may trivially derive the usual $7n + 1$ cluster electron pair count, since $7n + 1$ is the sum of $6n$ and $n + 1$, but we must note that this will often be modified in clusters with a single atom on the principal rotation axis (more examples appear in the next section). The $7n + 1$ rule is obeyed even by some clusters whose vertex atoms do not describe the surface of a sphere very well, for example $Pt_9(CO)_9(\mu_2\text{-}CO)_9^{2-}$ and $Pt_{15}(CO)_{15}(\mu_2\text{-}CO)_{15}^{2-}$,[22] although a particle on a cylinder analysis

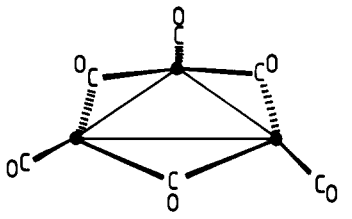

Figure 6. Idealized geometry of $Ni_3(CO)_6^{2-}$.

may be more appropriate for these molecules.[23]

In his calculations on $[Pt_3(CO)_6]_n^{2-}$ and $[Ni_3(CO)_6]_n^{2-}$ clusters using the chemical pseudopotential method,[24] Bullett identifies the HOMO as entirely carbonyl π^* in character.[25] However, we found that a Fenske–Hall calculation using the same idealized geometry for $Ni_3(CO)_6^{2-}$ (Figure 6) enabled all the TSH features discussed above to be identified. The HOMO is the latter calculation does have significant π^* character, but the important point is that the ligand–metal interaction alters the molecular orbital composition, not the symmetry-predicted electron count. In fact, the difference between the amounts of carbonyl π^* character found in the two calculations may be due to the non-Hermitian formulation involved in this pseudopotential method.[26]

The fluxionality of carbonyl ligands in many clusters is well-known experimentally, and is consistent with the theory, since the precise distribution of the ligands is clearly of secondary importance. The forces determining the exact distribution of carbonyls around a metal cluster have been the subject of some debate in the literature. Clearly the above theory is in accord with Johnson's argument that the arrangement is governed by packing forces between the ligands.[27] However, Evans' view that metal–carbonyl forces are most important[13] can also be investigated easily by using the TSH framework. He notes that in a triad such as Co, Rh, and Ir the member with the lowest atomic number tends to form clusters with bridging carbonyls, whereas the heavier metals do not. He cites $Co_4(CO)_9(\mu_2\text{-}CO)_3$ and $Ir_4(CO)_{12}$, in which the metal atoms both define tetrahedra, as examples. TSH theory in its simplest form predicts that these clusters will have the same electron count but that the cobalt cluster will have fewer electrons in "unhybridized" orbitals and more in metal–ligand σ bonds. Evans argues that the bridged structure is more favorable for Co because the Co d orbitals are less diffuse and are therefore more poorly stabilized by carbonyl π^* overlap. It seems likely that the correct viewpoint should take both of these effects into account and that electronic metal–ligand forces may discriminate between ligand arrangements with similar packing energies.

Application to Metallaboranes

Clearly the TSH method will reproduce the usual electron counts deduced by using the isolobal principle for simple metallaboranes. Examples include the family of clusters in which an $Fe(CO)_3$ fragment replaces a BH vertex. It will be more interesting to examine some species for which different bonding schemes have been proposed in the literature. Several cases are reviewed by Kennedy,[28] and we start with $(PPh_3)_2HIrB_8H_7Cl$ (Figure 7a). The skeletal geometry is similar to that of $B_9H_9^{2-}$ but is somewhat more open, with the Ir atom notionally replacing a four-coordinate vertex. An essential feature of TSH theory is that small changes in the arrangement of the vertices will generally be of minor importance in bonding considerations.[2,10] Hence we would expect to find the following accessible orbitals: seven B–H σ bonds, one B–Cl σ bond, three Ir–ligand bonds, three Ir "unhybridized" orbitals, and the cluster skeletal bonding orbitals. In this case the transition metal lies on a unique 2-fold rotation axis, and the nonbonding pair will be only approximately de-

(18) Woolley, R. G. *Nouv. J. Chim.* **1981**, *5*, 219, 227. Woolley, R. G. *Inorg. Chem.* **1985**, *24*, 3519, 3525.
(19) Wade, K. *J. Chem. Soc., Chem. Commun.* **1972**, 1974. Wade, K. *Adv. Inorg. Chem. Radiochem.* **1976**, *18*, 1. Williams, R. E. *Adv. Inorg. Chem. Radiochem.* **1976**, *18*, 67.
(20) Mingos, D. M. P.; Wales, D. J. *Introduction to Cluster Chemistry*; Prentice-Hall: Englewood Cliffs, NJ, in press.
(21) Wales, D. J. *Mol. Phys.* **1989**, *67*, 303.
(22) Schmidt, G. *Struct. Bonding* **1985**, *62*, 52.
(23) Zhenyang, L.; Mingos, D. M. P. *J. Organomet. Chem.* **1988**, *339*, 367.
(24) Fricker, H. S.; Anderson, P. W. *J. Chem. Phys.* **1971**, *55*, 5028, 5034. Chang, K. W.; Woolley, R. G. *J. Phys. C.* **1979**, *C12*, 2745.
(25) Bullett, D. W. *Chem. Phys. Lett.* **1985**, *115*, 450.
(26) Radtke, D. D.; Fenske, R. F. *J. Am. Chem. Soc.* **1967**, *89*, 2292.
(27) Johnson, B. F. G. *J. Chem. Soc., Chem. Comm.* **1976**, 211. Johnson, B. F. G.; Benfield, R. E. *J. Chem. Soc., Dalton Trans.* **1980**, 1743.
(28) Kennedy, J. D. *Prog. Inorg. Chem.* **1986**, *34*, 211.

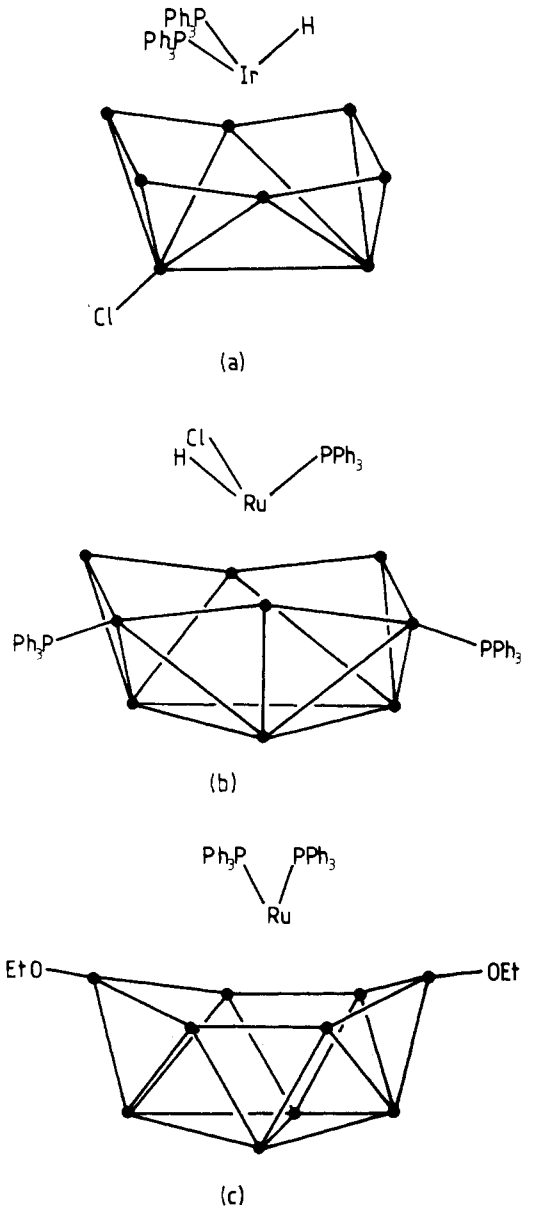

Figure 7. Structures of (a) $(PPh_3)_2HIrB_8H_7Cl$, (b) $(PPh_3)HClRuB_9H_7(PPh_3)_2$, and (c) $(PPh_3)_2RuB_{10}H_8(OEt)_2$. The metal atoms are shown isolated for clarity.

generate.[11] Of course, the axis is only a symmetry element for the skeletal atoms alone, but we would not expect the ligands to perturb the picture greatly in this case. The orbitals of the self-conjugate pair are expected to have appreciable amplitude at the unique atom on the principal axis, since the π cluster orbitals of this vertex span a nonbonding, self-conjugate E representation in idealized symmetry.[29] (The effect of a 2-fold axis is similar.[11]) Because the Ir atom is more electropositive than the boron atoms making up the other vertices, we expect the self-conjugate pair of orbitals to be destabilized relative to the other cluster orbitals. Hence n (i.e. 9) occupied cluster bonding orbitals are expected, not $n + 1$, and indeed this gives a total of 23 accessible orbitals, as required.

Two related examples are found in the 10- and 11-vertex isocloso compounds $(PPh_3)HClRuB_9H_7(PPh_3)_2$ and $(PPh_3)_2RuB_{10}H_8(OEt)_2$,[30] illustrated in Figure 7b,c. The electron

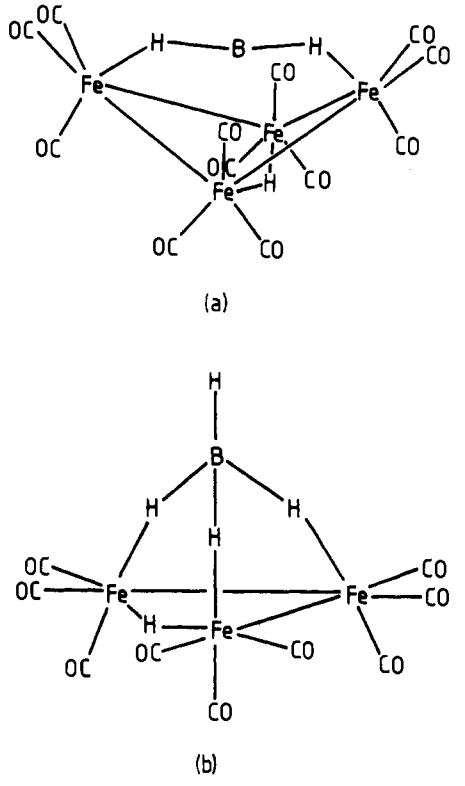

Figure 8. Structures of (a) $(\mu_2\text{-H})Fe_3(CO)_9(\mu_3\text{-}BH_4)$ and (b) $HFe_4(BH_2)(CO)_{12}$.

counts of these species may be understood in exactly the same way as above. The 10-vertex species has 50 valence electrons, which may be accommodated in 7 B–H σ bonds, 2 B–PPh_3 σ bonds, 3 Ru "unhybridized" orbitals, 3 Ru–ligand bonds and 10 cluster bonding orbitals. The n skeletal orbitals may be described in the same way as above. Similarly the 11-vertex compound has 54 valence electrons, which may be accommodated in 8 B–H σ bonds, 2 B–OEt σ bonds, 2 Ru–PPh_3 bonds, 4 "unhybridized" Ru orbitals, and 11 cluster bonding orbitals. The novel 10-vertex isocloso species $H(PPh_3)(Ph_2PC_6H_4)IrB_9H_8$[28] also conforms to this scheme, as the reader may demonstrate.

Kennedy and his co-workers have favored an alternative bonding scheme for all three of the above molecules in which the metal atom makes a four-orbital contribution to the cluster bonding. However, this clearly does not fit with the three-cluster-hybrid rule based upon the TSH theory description, which is closer to Baker's hypercloso description.[31] Further evidence is provided by the simple explanation of the n skeletal electron pairs provided by TSH theory and some recent calculations.[32] The scheme is particularly compelling when there is an idealized 3-fold rotation axis or higher, as the pairing principle then indicates that either three or five metal orbitals could be used for skeletal bonding. For 8-, 9-, and 11-vertex hypercloso clusters where there is only an idealized 2-fold axis the analysis is less clear-cut.

However, the argument can be made more convincing by considering molecules that have a single main-group cluster atom and transition-metal atoms at the other vertices. If the main-group atom lies on the principle rotation axis in such a molecule, we would now expect the two approximately nonbonding orbitals localized partly on this more electronegative vertex to be stabilized relative to the other frontier orbitals. Hence $n + 2$ skeletal electron pairs are likely in these species.

We consider two recently synthesized species as examples:[33] $(\mu_2\text{-H})Fe_3(CO)_9(\mu_3\text{-}BH_4)$ and $HFe_4(BH_2)(CO)_{12}$, which are il-

(29) Wales, D. J. Submitted for publication.
(30) Crook, J. E.; Elerington, M.; Greenwood, N. N.; Kennedy, J. D.; Woollins, J. D. *Polyhedron* **1984**, *3*, 901. Crook, J. E.; Elerington, M.; Greenwood, N. N.; Kennedy, J. D.; Thornton-Pett, M.; Woollins, J. D. *J. Chem. Soc., Dalton Trans.* **1985**, 2407. Bould, J.; Crook, J. E.; Greenwood, N. N.; Kennedy, J. D.; McDonald, W. S. *J. Chem. Soc., Chem. Commun.* **1982**, 353.
(31) Baker, R. T. *Inorg. Chem.* **1986**, *25*, 109.
(32) Johnston, R. L.; Mingos, D. M. P. *Inorg. Chem.* **1986**, *25*, 3321.
(33) Wong, K. S.; Scheidt, W. R.; Fehlner, T. P. *J. Am. Chem. Soc.* **1982**, *104*, 1111. Fehlner, T. P.; Housecraft, C. E.; Scheidt, W. R.; Wong, K. S. *Organometallics* **1983**, *2*, 825. Vites, J. C.; Eigenbrot, C.; Fehlner, T. P. *J. Am. Chem. Soc.* **1984**, *106*, 4633.

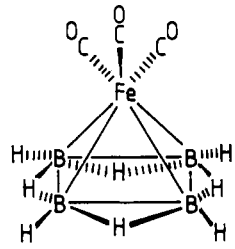

Figure 9. Structure of $Fe(CO)_3B_4H_8$.

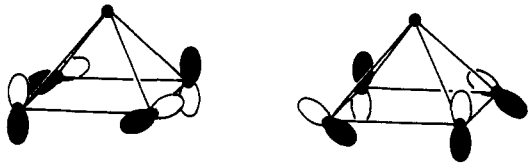

Figure 10. The two nonbonding e orbitals of a nido-square-based pyramid. Note that they are related by the TSH theory pairing operation.

lustrated in parts a and b of Figure 8 respectively. The valence electron count for the tetrahedral species is 50, which may be accommodated in 9 Fe–(CO) bonds, 9 Fe "unhybridized" orbitals, one B–H σ bond and $n + 2 = 6$ cluster bonding orbitals. The tetrahedron is unusual in that all vertices are three-coordinate, and hence an edge-bonding scheme is possible in which the three cluster hybrids per vertex are directed toward the three nearest neighbours. The fact that the four bridging hydrogen atoms lie directly over four edges of the notional tetrahedron almost certainly indicates that these are regions of high electron density.

For the five-vertex species there are 62 valence electrons, which may be accommodated in 12 Fe-CO bonds, 12 Fe "unhybridized" orbitals and $n + 2 = 7$ cluster bonding orbitals. In a previous study, this molecule was considered as an arachno fragment with the boron atom essentially interstitial. The alternative view with the cluster atoms describing a trigonal bipyramid is more suited to the present purpose and probably makes the electron count easier to understand.

As a final example of this type we note that $Fe_4C(CO)_{12}^{2-}$ may be viewed as an arachno octahedron of iron atoms with an interstitial carbon atom in the usual manner.[34] However, it also fits into the above scheme when considered as a closo cluster with a more electronegative carbon atom on the principle axis.

Some readers may wonder whether $Fe(CO)_3B_4H_8$ is consistent with the above picture, since it has a single cluster atom (iron) on the 4-fold principal axis and the usual nido electron count (Figure 9). In fact, the bonding in this molecule may be understood by using precisely the same approach: it is a five-vertex cluster with a single atom on the principal axis and is therefore expected to have five or seven bonding cluster orbitals. Above we reasoned that molecules of the isocloso series would have n skeletal electron pairs because the two approximately nonbonding orbitals would be destabilized relative to the other frontier orbitals. For $Fe(CO)_3B_4H_8$, the argument is modified because this is a nido species, and we expect the "missing" BH vertex to interact strongly with the self-conjugate e pair of the orbitals in question.[2] It follows that these e orbitals are mainly localized around the open face of the square-based pyramidal molecule, not on the iron atom (Figure 10).[29,35] Hence, the $n + 2$ occupied skeletal orbitals are consistent with the arguments of the preceding paragraphs. A systematic analysis of the TSH pairing principle and energy level patterns in clusters is presented elsewhere.[29]

Hence, we have shown that all the above species can be understood in terms of the three-cluster-hybrid rule deduced from TSH theory. As Greenwood observes,[36] other authors have suggested bonding schemes for various metallaboranes in which metal centers contribute anywhere between one and four orbitals

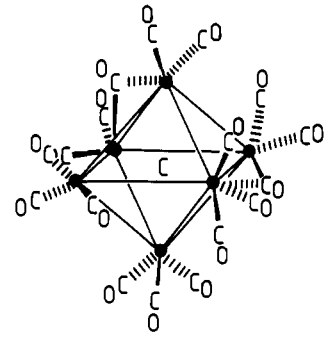

Figure 11. Structure of $Ru_6(CO)_{17}C$.

to the cluster bonding. Molecules for which such schemes are really necessary are expected to be identifiable as species in which one or more of the fundamental assumptions of TSH theory breaks down. This may be because they are too open or because the assumption that the six orbitals per metal atom which are not involved in cluster bonding will all correlate with accessible orbitals does not hold. The large energy gap between the np and $(n - 1)$d orbitals in platinum and gold means that clusters of these elements may also deviate from the usual rules.

The three-cluster-hybrid rule clearly works best for clusters with closed (or nearly closed) skeletons, as discussed in detail elsewhere.[21] Further, since TSH theory in its simplest form does not distinguish between different metal atoms in considering the electron count, it clearly cannot hope to cope with cases where the count probably depends on the identity of the particular metal involved. More detailed considerations are required in such cases.

Large Clusters and Interstitial Atoms

The first step toward an understanding of larger transition-metal clusters must be a consideration of interstitial atoms. A qualitative TSH description of the effects of interstitial atoms has already been given.[7] To investigate such species in a more quantitative fashion, a Fenske–Hall calculation was performed on $Ru_6(CO)_{17}C$ (Figure 11) in an idealized approximation to the experimental geometry[37] with Ru–Ru = 2.9 Å, Ru–CO = 2.05 Å, C–O = 1.17 Å, and OC–Ru–CO = 90°. The results support Stone's earlier conclusion that the valence orbitals of the interstitial atom do not produce any additional accessible orbitals, and that there are simply $7n + 1$ occupied orbitals. The carbon 2s and 2p orbitals mix mostly with the S_d^σ and P_d^σ orbitals to give bonding (accessible) and antibonding (inaccessible) combinations. These cluster orbitals were illustrated in Figure 1 for s basis functions. Since the L_d^σ orbitals are considered to be part of the "unhybridized" occupied set in the previous examples, we can see that no change results in the number of formally accessible orbitals. Interaction with inwardly hybridized *inaccessible* L^σ orbitals would be expected to produce new accessible orbitals. However, the L_d^σ orbitals are much nearer in energy to the interstitial orbitals, and mixing between these functions is greatest, in agreement with an extended Hückel calculation on the same species.[34] Hence, the interstitial atoms provide additional electrons but no more accessible orbitals and are therefore an excellent remedy for electron deficiency in transition-metal clusters. One need look no further than the bulk metallic limit to see an extreme illustration of this idea.

Although this calculation is again useful for comparison with theory, the detailed results should not be taken too seriously. For example, the final Mulliken atomic charge on the interstitial carbon atom is found to be −0.82, and there are appreciable changes in the character of the frontier orbitals. Because the method involves a one-electron SCF approximation, it is likely to overestimate the charge polarization involved because electron correlation is neglected.

$Os_{10}C(CO)_{12}(\mu_2\text{-}CO)_{12}^{2-}$,[38] whose cluster skeleton is illustrated in Figure 12, is a more complicated example. This molecule may

(34) Wijeyesekera, S. D.; Hoffmann, R. *Organometallics* **1984**, *3*, 975.
(35) Mingos, D. M. P.; Zhenyang, L., *Struct. Bonding*, in press.
(36) Greenwood, N. N. *Chem. Soc. Rev.* **1984**, *13*, 353.
(37) Sirigu, A. *J. Chem. Soc., Chem. Commun.* **1969**, 596.
(38) Jackson, P. F.; Johnson, B. F. G.; Lewis, J.; Nelson, W. H. *J. Chem. Soc., Dalton Trans.* **1982**, 2099.

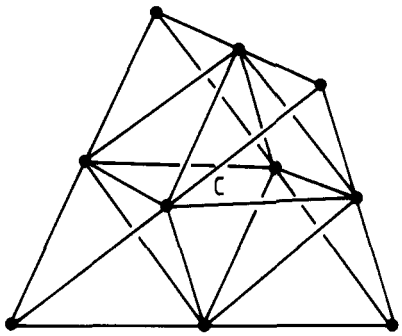

Figure 12. Cluster skeleton of $Os_{10}C(CO)_{12}(\mu_2\text{-}CO)_{12}^{2-}$.

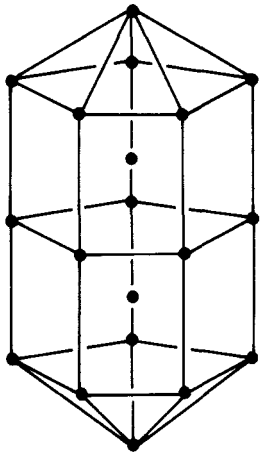

Figure 13. Cluster skeleton of $Pt_{19}(CO)_{12}(\mu_2\text{-}CO)_{10}^{2-}$.

be considered as an octahedron of Os atoms, with four faces tetrahedrally capped by conical $Os(CO)_3$ fragments; the interstitial carbon atom lies in the central octahedral chamber. This molecule has 134 valence electrons, which may be accommodated in $7n + 1 = 43$ orbitals formally associated with the Os_6 octahedron plus 12 Os–CO bonds and 12 "unhybridized" orbitals associated with the $Os(CO)_3$ caps. Here the electron count for the octahedron includes 12 orbitals that may be viewed as edge-bonds to the four $Os(CO)_3$ caps, in line with King's approach to large rhodium carbonyl clusters.[39]

What does the theory have to say about even larger metal clusters that may contain more than one interstitial atom?[22,40] First, consider $Pt_{19}(CO)_{12}(\mu_2\text{-}CO)_{10}^{2-}$,[41] whose skeleton is illustrated in Figure 13. This molecule has 238 valence electrons, 2 short of the number required to fill $7n + 1 = 120$ orbitals, where $n = 17$ is the number of platinum atoms in the cage. Careful consideration of the mixing between orbitals of the interstitial atoms and the surface atoms is needed to explain the detailed electron counts of a wide variety of high nuclearity clusters,[42] and we will illustrate the method for the above species. The two interstitial atoms, considered as a dimeric unit, have a total of 16 orbitals that can interact significantly with the n_s $L^{\pi}_{p/d}$ skeletal bonding orbitals of the $n_s = 17$ atoms in the outer shell. This gives 16 bonding orbitals, with one of the $L^{\pi}_{p/d}$ levels "left over" and inaccessible because of the high 6p atomic orbital energy in platinum. The S^{σ} orbital interacts strongly with the dimer σ bonding orbital to give strongly bonding and antibonding combinations and a total of 17 skeletal bonding orbitals, i.e. 1 less than the usual $n_s + 1$. We should also note that there are several species, such as $Pt_{26}(CO)_{23}(\mu_2\text{-}CO)_9^{2-}$, with three interstitial platinum atoms, that do not conform to either of the cases identified by Mingos as "radial" and "tangential".

$Au_{55}(PPh_3)_{12}Cl_6$ and $Rh_{55}(PPh_3)_{12}Cl_6$ deviate even more strongly from naive expectations.[43] Schmidt[22] presents evidence to suggest that the gold cluster consists of one central gold atom surrounded by a cuboctahedron of 12 gold atoms, which in turn is surrounded by a shell of 42 more gold atoms. This arrangement suggests that a "Russian doll" model might be applicable, in which we count the inwardly hybridized cluster bonding orbitals of the inner shell as well as the outer. This model is based on the reasonble assumption that the inwardly hybridized orbitals of the inner shell will not interact strongly with those of the outer shell. However, when we note that the Rh cluster has 110 fewer electrons, it becomes clear that the electron count depends strongly on the particular transition metal in these species. A limit has therefore been reached where the orbitals are so densely spaced that the electron count will probably depend upon how many carbonyls or other ligands can be found to the limited surface area. This is hardly surprising, for as the size of the metallic fragment increases, we would expect it to begin to behave more like a piece of bulk metal with a variable number of adsorbed carbonyls.

We can estimate where the TSH theory in this form may cease to be useful. This can be compared with the results of other authors who have addressed the question of when a transition-metal cluster begins to "look" more like a metallic fragment.[44] First, note that the TSH cluster orbitals have an associated "quantum number", L, pertaining to the spherical harmonic, Y_{LM}, from which the expansion coefficients in the LCAO wave function are derived. For further details of the generation of the expansion coefficients the reader is referred elsewhere.[10] We have previously estimated the critical value of L, L_c, for which axial π cluster orbitals will become bonding in a regular polyhedron of coordination number λ. The result is[10]

$$L_c \geq \lambda/2$$

For a spherical shell of n atoms there are $2n$ π-type cluster orbitals with associated L quantum numbers 1, 2, ..., L_m, where L_m is approximately given by

$$\sum_{L=1}^{L_m} (2L + 1) = n$$

That is, $(L_m + 1)^2 - 1 = n$, or $L_m = (n + 1)^{1/2} - 1$. Hence, we expect the polar and axial π cluster orbitals to overlap when $(n + 1)^{1/2} - 1 \approx \lambda/2$. Since the largest coordination number observed in practice for an atom within a single cluster shell is 6, this implies that overlap is likely to begin for clusters with about 15 atoms in a single shell. When overlap begins to occur, a qualitative TSH treatment will no longer give a good idea of the number of cluster bonding orbitals because the L^{π} and $\bar{L}^{\pi}$ sets are not clearly separated in energy. However, the limit described above assumes that all the skeletal atoms lie on the surface of a sphere. This is clearly not a very good approximation for some of the above species, and there are also a number of approximations involved in the estimate of L_c.

The above analysis leads us to recognize two distinct regimes. For bulk metals, we know that the wave vector in momentum space provides a useful approximate quantum number for classifying the eigenstates and eigenfunctions. This limit is the domain of metal physics. However, for smaller transition-metal clusters the symmetry-based classification of TSH theory provides the most useful approximate quantum number, namely L. This quantum number actually corresponds to the orbital angular momentum of an electron about the center of the cluster, which we assume throughout to be approximately spherical. The periodicity of the bulk lattice in the limit of large fragments determines the most appropriate approximate quantum numbers to use in this case. In between these limits, neither classification may be particularly

(39) King, R. B. *Inorg. Chim. Acta* **1986**, *116*, 125.
(40) Chini, P. *J. Organomet. Chem.* **1980**, *200*, 37.
(41) Washecheck, D. M.; Wucherer, E. J.; Dahl, L. F.; Ceriotti, A.; Longani, G.; Manassero, M.; Sansoni, M.; Chini, P. *J. Am. Chem. Soc.* **1979**, *101*, 6110.
(42) Mingos, D. M. P.; Zhenyang, L. *J. Chem. Soc., Dalton Trans.* **1988**, 1657.
(43) Mingos, D. M. P. *J. Chem. Soc., Dalton Trans.* **1976**, 1163. King, R. B. *Inorg. Chim. Acta* **1986**, *116*, 109. Mingos, D. M. P. *J. Organomet. Chem.* **1984**, *268*, 275.
(44) Demuynck, J.; Rohmer, M.; Strich, A.; Veillard, A. *J. Chem. Phys.* **1981**, *75*, 3443. Datta, N. C.; Sen, B. *J. Chem. Soc., Faraday Trans. 2* **1986**, *82*, 977.

helpful. We are then left with the familiar problem of full diagonalization of the Hamiltonian without knowledge of any basis functions that achieve partial blocking.

Summary

In this paper, we have investigated the detailed application of tensor surface harmonic theory to the structure and bonding of transition-metal clusters and related species. We have shown that a simple, unified treatment may be applied despite the large number of orbitals involved. The proposed scheme has firm group-theoretical foundations, and is shown to encapsulate the ideas of the isolobal principle. When combined with other TSH results, the theory can rationalize the electron counts of a diverse range of species, including metallaboranes and transition-metal clusters with a single main-group atom in the skeleton. We have also discussed the use of TSH theory to investigate the electron counts of very large metal clusters.

The main advantage of the method is that it enables generalized electron counting rules to be deduced from firm theoretical principles. Such derivations are particularly straightforward for closo deltahedra. More detailed treatments also enable us to rationalize the bonding in nido and arachno species and in large transition-metal cluster carbonyls with interstitial moieties. Such structure–electron count correlations are useful in making predictions about real chemical reactions.[20] For example, the disposition of the nonbonding orbital in polar clusters helps us to rationalize deviations from the usual electron-counting rules and predict reactivity.

Further applications to the theoretical study of fluxional processes in both main-group and transition-metal clusters[11] may be of great importance in future work. Recent developments include the development of a qualitative center-of-gravity rule for the splitting of cluster orbitals,[45] a tensor solid harmonic theory for multishell clusters, more detailed studies of cluster hybridization[21] and the pairing principle,[29] and the use of TSH theory in the interpretation of cluster NMR data.[46]

Acknowledgment. We wish to thank Dr. R. G. Woolley and Dr. D. M. P. Mingos for their useful comments on the manuscript, Dr. Catherine Housecroft for some helpful discussions, and the SERC for financial support.

(45) Wales, D. J.; Mingos, D. M. P. *Inorg. Chem.*, in press.
(46) Wales, D. J.; Mingos, D. M. P. Manuscript in preparation.

Contribution from the Departments of Chemistry, University of Denver, Denver, Colorado 80208, and University of Colorado at Denver, Denver, Colorado 80204

Metal-Nitroxyl Interactions. 54. EPR Spectra of High-Spin Iron(III) Complexes of Spin-Labeled Tetraphenylporphyrins in Frozen Solution

Lee Fielding, Kundalika M. More, Gareth R. Eaton,* and Sandra S. Eaton*

Received December 15, 1988

Frozen-solution EPR spectra were obtained for high-spin iron(III) complexes of seven ortho-spin-labeled tetraphenylporphyrins and four iron(III) porphyrin complexes with nitroxyl carboxylates as axial ligands. Data obtained at 5–12 K provided examples of iron–nitroxyl spin–spin interactions ranging from small perturbations of the iron and nitroxyl line widths to $|J| = 0.17$ cm^{-1}. Increasing iron relaxation rates at higher temperatures caused collapse of the spin–spin splittings due to interactions with $|J| < \sim 0.05$ cm^{-1}. Multiple conformations with different magnitudes of spin–spin interaction were observed for the complexes of the ortho-spin-labeled porphyrins. Six-coordination of the iron or π complexation of the porphyrin ring favored population of the conformations with weaker electron–electron spin–spin interaction. The stronger electron–electron spin–spin interactions are assigned to conformations with weak orbital overlap between the ortho substituent and orbitals of the porphyrin π system or the metal.

Introduction

Interpretations of EPR spectra obtained for biological samples including photosynthetic systems,[1,2] spin-labeled cytochrome P450,[3,4] and spin-labeled iron transferrin[5] have invoked electron–electron spin–spin interaction between organic radicals and paramagnetic iron centers.[6] Analysis of spectra of this type could be facilitated by comparison with data for small molecules that demonstrate the effects of interaction between paramagnetic iron(III) and organic radicals on the EPR spectra. Studies are therefore under way to characterize these effects.

A series of spin-labeled iron porphyrins (I–XI, Chart I) were selected to provide a range of strengths of the iron–nitroxyl spin–spin interaction. In I–VII the length of the ortho substituent between the porphyrin and the nitroxyl rings was varied. Frozen-solution EPR spectra of the low-spin iron(III) complexes $Fe(P)L_2$, P = I–VII, L = imidazole or 1-methyl-imidazole, provided examples of spectra due to exchange interaction up to 0.28 cm^{-1} and provided a basis for interpretation[7] of the previously reported spectra for spin-labeled cytochrome P450. The fluid-solution EPR spectra of high-spin VIII–XI and Fe(P)X, P = I–VII, X = F^-, Cl^-, Br^-, I^-, demonstrated that the nitroxyl signal broadened and shifted to higher g value as the strength of the iron–nitroxyl spin–spin interaction increased.[8] We now report EPR studies of high-spin VIII–XI and of the high-spin iron(III) complexes of spin-labeled porphyrins I–VII in frozen solution.

Experimental Section

Physical Measurements. X-Band EPR spectra were obtained on a Varian E9 spectrometer interfaced to a Varian 620/L103 or IBM C-S9000 laboratory computer or on an IBM ER200 spectrometer interfaced to an IBM CS9000 computer. The lines in most of the EPR spectra were sufficiently broad that the spectra were unchanged by degassing. Therefore, the spectra discussed below were obtained on air-saturated samples unless otherwise noted. Sample concentrations were about 1 mM except for experiments designed to check for concentration dependence. All spectra were obtained at microwave powers that did not cause saturation of the signal and with 100-kHz modulation at amplitudes that did not distort the line shapes. Quantitation of the nitroxyl EPR signals was done by comparison of the double integrals of the spectra with double integrals for solutions of known concentrations of 2,2,6,6-tetramethylpiperidin-1-yl or 4-oxo-2,2,6,6-tetramethylpiperidin-1-yl in the same

* To whom correspondence should be addressed: G.R.E., University of Denver; S.S.E., University of Colorado at Denver.

(1) Ito, S.; Tang, X. S.; Sato, K. *FEBS Lett.* **1986**, *205*, 275.
(2) Beijer, C.; Rutherford, A. W. *Biochim. Biophys. Acta* **1987**, *890*, 169.
(3) Pirrwitz, J.; Lassman, G.; Rein, H.; Ristau, O.; Janig, G. R.; Ruckpaul, K. *FEBS Lett.* **1977**, *83*, 15.
(4) Pirrwitz, J.; Lassman, G.; Rein, H.; Janig, G. R.; Pecar, S.; Ruckpaul, K. *Acta Biol. Med. Ger.* **1979**, *38*, 235.
(5) Najarian, R. C.; Harris, D. C.; Aisen, P. *J. Biol. Chem.* **1978**, *253*, 38.
(6) Eaton, S. S.; Eaton, G. R. *Biol. Magn. Reson.*, in press.
(7) Fielding, L.; More, K. M.; Eaton, G. R.; Eaton, S. S. *J. Am. Chem. Soc.* **1986**, *108*, 618.
(8) Fielding, L.; More, K. M.; Eaton, G. R.; Eaton, S. S. *Inorg. Chem.* **1987**, *26*, 856.

0020-1669/89/1328-3127$01.50/0